

Org Lett. Author manuscript; available in PMC 2013 September 07.

Published in final edited form as:

Org Lett. 2012 September 7; 14(17): 4442-4445. doi:10.1021/ol3019456.

# Stereoselective Synthesis of Acortatarins A and B

Jacqueline M. Wurst<sup>†</sup>, Alyssa L. Verano<sup>‡</sup>, and Derek S. Tan<sup>†,‡,§</sup>

Derek S. Tan: tand@mskcc.org

<sup>†</sup>Tri-Institutional Training Program in Chemical Biology, Memorial Sloan–Kettering Cancer Center, 1275 York Avenue, Box 422, New York, NY 10065

<sup>‡</sup>Pharmacology Program, Weill Cornell Graduate School of Medical Sciences, Memorial Sloan–Kettering Cancer Center, 1275 York Avenue, Box 422, New York, NY 10065

§Molecular Pharmacology & Chemistry Program and Tri-Institutional Research Program, Memorial Sloan–Kettering Cancer Center, 1275 York Avenue, Box 422, New York, NY 10065

### **Abstract**

Acortatarins A and B have been synthesized via stereoselective spirocyclizations of glycals. Mercury-mediated spirocyclization of a pyrrole monoalcohol sidechain leads to acortatarin A. Glycal epoxidation and reductive spirocyclization of a pyrrole dialdehyde sidechain leads to acortatarin B. Acid equilibration and crystallographic analysis indicate that acortatarin B is a contrathermodynamic spiroketal with distinct ring conformations compared to acortatarin A.

Acortatarins A and B are novel spiroketal pyrrole alkaloids from the roots of *Acorus tatarinowii* (Figure 1). Structurally related pollenopyrrosides A and B were isolated contemporaneously from the pollen of *Brassica campestris*. Notably, acortatarins A and B exhibited significant antioxidant activity in a renal cell model for hyperglycemia-induced production of reactive oxygen species (ROS). Thus, these natural products are potential starting points for the development of new therapeutics to treat diabetic complications, cancer, and other conditions in which ROS are implicated. However, due to low isolation yields from the natural sources, efficient synthetic routes are needed to enable detailed biological evaluation. Herein, we report concise, modular syntheses of acortatarins A and B via stereoselective spirocyclizations of glycals. The thermodynamic preferences of both spiroketal natural products and the crystal structure of acortatarin B are also described.

In the original isolation paper, the relative configuration of acortatarin A was established by crystallography and an unnatural absolute L-configuration was assigned based on Mosher analysis. An α-*ribo* relative configuration was assigned to acortatarin B based on ROESY analysis and the L-configuration assumed by analogy. Notably, pollenopyrroside B was separately assigned the enantiomeric D-configuration of acortatarin A based on crystallographic analysis of its pyranose congener pollenopyrroside A (not shown).<sup>2</sup>

Subsequently, Sudhakar reported the first total syntheses of acortatarins A and B from 2-deoxy-p-ribose and p-arabinose, respectively, leading to structural revisions of both absolute configurations as well as the relative configuration of acortatarin B (Figure 1). Thus, acortatarin A and pollenopyrroside B are now recognized to be identical. A second synthesis of acortatarin A from p-mannitol was also reported recently by Brimble. These reports provide the first synthetic access to the acortatarins, but their practical utility is limited by low overall yields and reliance upon classical acid-catalyzed spiroketalization reactions that afford low or even undesired diastereoselectivity.

Our laboratory has a long-standing interest in the stereocontrolled synthesis of spiroketals from glycals, <sup>8, 9, 10</sup> and we envisioned that both acortatarins A and B could be synthesized by spirocyclizations of glycals **1** (Figure 2). Direct spirocyclization would provide acortatarin A while epoxidation–spirocyclization would lead to acortatarin B. In the latter case, we recognized that the oxidation state of the pyrrole substituents would be important for enabling chemoselective epoxidation of the glycal. These key intermediates **1** would originate from coupling of appropriate pyrroles **2** with ribal derivative **3**, accessed via nucleobase elimination of thymidine. <sup>11</sup> At the outset of our studies, the revised structures of the acortatarins had not been reported but, recognizing that both enantiomers of thymidine are commercially available, initial work was carried out with the less expensive, natural prongener.

Thus, TIPS-protected<sup>12</sup> ribal **6**<sup>11</sup> underwent C1-formylation<sup>13</sup> and reduction to provide hydroxymethyl ribal **7**, which was then converted to iodide **8** (Figure 3).<sup>14</sup> The pyrrole dicarboxaldehyde **9**<sup>15, 16</sup> was then coupled under biphasic conditions<sup>17</sup> to afford the key pyrrologlycal **10**.

To access acortatarin A, we initially attempted reductive spirocyclization of dialdehyde 10 (TFA, Et<sub>3</sub>SiH), envisioning cyclization of an aldehyde carbonyl followed by *in situ* reduction of the resulting spirocyclic oxocarbenium intermediate, but this led to a furan side product via Ferrier-type elimination (Figure S1). Similarly, stepwise reduction to monoalcohol 11 (Figure 4) followed by treatment with dichloroacetic acid led to a 1:1 mixture of a 2,3-dehydro- $\alpha$ -spiroketal (*cf.* 12) via Ferrier rearrangement and the undesired  $\beta$ -spiroketal 13.  $\alpha$ 

Thus, we next investigated oxidative spirocyclizations of pyrrole monoalcohol **11** that would yield spiroketals having a removable C2-substituent, and were delighted to find that treatment with Hg(II) salts afforded the desired 2-mercurial spiroketals, which were then reduced with NaBH<sup>4</sup> to afford the diastereomeric spiroketals **12** and **13**. <sup>9d</sup> Initial reactions with Hg(OAc)<sub>2</sub> or Hg(TFA)<sub>2</sub> led to modest stereoselectivity favoring the desired  $\alpha$ -spiroketal **12** (Table 1, entries 1–5). Notably, Hg(TFA)<sub>2</sub> resulted in 30% formation of the same Ferrier rearrangement-derived 2,3-dehydro- $\alpha$ -spiroketal observed above (entry 2).

The  $Hg(OAc)_2$ -derived 2-mercurial spiroketals exhibited a 7.8 Hz C2-H/C3-H coupling constant, consistent with a 2,3-*trans* relationship arising from  $\beta$ -mercuration (Figure S2). <sup>16</sup> Since the expected *anti*-oxymercuration would then lead to the desired  $\alpha$ -spiroketal 12, <sup>18</sup> we postulate that the undesired  $\beta$ -spiroketal 13 arises from net *syn*-oxymercuration via an oxocarbenium intermediate. Thus, to accelerate *anti*-oxymercuration, pyrrole monoalcohol 11 was pretreated with NaHMDS to form a more reactive alkoxide nucleophile, resulting in increased stereoselectivity for the desired  $\alpha$ -spiroketal 12 (entry 7). Surprisingly, however, longer reaction times prior to NaBH<sub>4</sub> reduction led to further increased stereo-selectivity, indicative of an unanticipated equilibrium effect in this reaction (entries 6–10). Such equilibration was not observed without base, <sup>16</sup> and other bases provided comparable or

lower stereoselectivity. <sup>16</sup> Desilylation of the mixture of **12** and **13** then provided the separable acortatarin A (**14**) and C1-*epi*-acortatarin A (**15**). <sup>16</sup>, <sup>19</sup>

Next, we pursued an epoxidation–spirocyclization approach to acortatarin B. <sup>91</sup> In initial epoxidation studies, pyrrole monoalcohol **11** and its diol congener (not shown) were prone to pyrrole oxidation. In contrast, pyrrole dicarboxaldehyde **10** underwent chemoselective  $\beta$ -epoxidation of the glycal with DMDO to form the putative epoxide **16** (Figures 5 and S3). <sup>16</sup> Addition of NaBH<sup>4</sup> in MeOH afforded the  $\alpha$ -spiroketal methanol adduct **22a** (Table 2, entry 1). In contrast, NaBH<sub>4</sub> in THF provided the desired  $\beta$ -spiroketal **17** as a single diastereomer, along with a tetracyclic side product **21** (entry 2). Attempted ionic reduction with Et<sub>3</sub>SiH resulted only in tetracycle **21** (entry 3). Conversely, reductive spirocyclization with acidic NaBH<sub>3</sub>CN yielded the epimeric  $\alpha$ -spiroketal **18** and tetracycle **21** (entry 4). NaBH(OAc)<sub>3</sub> led to  $\alpha$ -spiroketal acetate adduct **22b** (entry 5) while LiEt<sub>3</sub>BH and L-Selectride yielded complex mixtures (entries 6,7). Finally, Bu<sub>4</sub>NBH<sub>4</sub>, aided by its solubility in CH<sub>2</sub>Cl<sub>2</sub>, provided the desired  $\beta$ -spiroketal **17** in excellent yield and diastereoselectivity (entries 8, 9). Spiroketals **17** and **18** were seperable and desilylation provided acortatarin B (**19**) and its C1-epimer (**20**). <sup>16, 20</sup>

We next investigated acid-catalyzed equilibration of the natural products and their unnatural C1-anomers, as well as the TIPS-protected congeners (12–15, 17–20). <sup>21</sup> In both series, the  $\alpha$ -spiroketal was favored by a 65:35 ratio (Figures 4, 5). <sup>16</sup> Notably, this favors the unnatural anomer of acortatarin B. Accordingly, although it is commonly assumed that spiroketal biosynthesis is a spontaneous, thermodynamically-controlled process, acortatarin B is a contrathermodynamic spiroketal whose biosynthesis may be under enzymatic stereocontrol. <sup>22</sup>, <sup>23</sup>

Finally, we obtained a crystal structure of acortatarin B for comparison to the reported structure of acortatarin A (Figure 6). Interestingly, acortatarins A and B adopt distinct furanose envelope conformations ( $E_1$  vs.  $E_2$ ) and morpholine half-chair conformations ( $^{\rm O}H_1$  vs.  $^{\rm I}H_0$ ) to allow double anomeric stabilization in both systems.

In conclusion, we have developed efficient, stereocontrolled syntheses of acortatarins A and B from a key pyrrologlycal **10**. Acortatarin A was synthesized in 9 steps and 30% overall yield from p-thymidine, with 9:1 diastereoselectivity at the spiroketal-forming step and acortatarin B was accessed in 8 steps and 41% overall yield with complete diastereoselectivity. This compares favorably to previous syntheses<sup>7</sup> and provides practical access to the natural products and a variety of analogues. Mechanistic analysis of the opposite stereoselectivities observed in these two spirocyclizations and biological studies are ongoing and will be reported in due course.

## **Supplementary Material**

Refer to Web version on PubMed Central for supplementary material.

### **Acknowledgments**

We thank Prof. Yong-Xian Cheng (Kunming Institute) for providing samples of the acortatarins, Dr. George Sukenick, Dr. Hui Liu, Hui Fang, and Dr. Sylvi Rusli (MSKCC) for expert NMR and mass spectral support, Dr. Kristen Kirschbaum (U. Toledo) for X-ray crystallographic analysis, and the NIH (P41 GM076267, T32 CA062948-Gudas) for financial support.

#### References

1. Tong X-G, Zhou L-L, Wang Y-H, Xia C, Wang Y, Liang M, Hou F-F, Cheng Y-X. Org. Lett. 2010; 12:1844–1847. [PubMed: 20329735]

- Guo J-L, Feng Z-M, Yang Y-J, Zhang Z-W, Zhang P-C. Chem. Pharm. Bull. 2010; 58:983–985.
   [PubMed: 20606352]
- 3. Valko M, Leibfritz D, Moncol J, Cronin MTD, Mazur M, Telser J. Int. J. Biochem. Cell Biol. 2007; 39:44–84. [PubMed: 16978905]
- 4. 50 kg *A. tatarinowii* root yielded 7.3 mg acortatarin A and 3.4 mg acortatarin B (ref 1); 15 kg *B. campestris* pollen yielded 6 mg pollenopyrroside A and 5 mg pollenopyrroside B (ref 2).
- Sudhakar G, Kadam VD, Bayya S, Pranitha G, Jagadeesh B. Org. Lett. 2011; 13:5452–5455.
   [PubMed: 21955040]
- 6. Geng HM, Chen JL-Y, Furkert DP, Jiang S, Brimble MA. Synlett. 2012; 23:855–858.
- 7. Ref 5 provides acortatarin A in 3.7% over 10 steps, with the key spirocyclization proceeding in 1.4:1 diastereoselectivity; accounting for epimerization of both anomers in a subsequent step to a 9:1 mixture favoring the desired diastereomer, the overall yield increases to 6.4%. Acortatarin B is accessed in 0.9% yield over 10 steps, with the key spirocyclization proceeding in 1:4.6 unfavorable diastereoselectivity. Ref 6 provides acortatarin A in 1.7% yield over 13 steps, with the key spirocyclization proceeding in 1.5:1 diastereoselectivity.
- (a) Potuzak JS, Moilanen SB, Tan DS. J. Am. Chem. Soc. 2005; 127:13796–13797. [PubMed: 16201793] (b) Moilanen SB, Potuzak JS, Tan DS. J. Am. Chem. Soc. 2006; 128:1792–1793. [PubMed: 16464069] (c) Liu G, Wurst JM, Tan DS. Org. Lett. 2009; 11:3670–3673. [PubMed: 19634891] (d) Wurst JM, Liu G, Tan DS. J. Am. Chem. Soc. 2011; 133:7916–7925. [PubMed: 21539313]
- 9. For selected early studies on the synthesis of spiroketals from cyclic enol ethers, see: Knabe J, Schaller K. Arch. Pharm. 1968; 301:457–464. Clark-Lewis JW, McGarry EJ. Aust. J. Chem. 1975; 28:1145–1147. Boeckman RK Jr, Bruza KJ, Heinrich GR. J. Am. Chem. Soc. 1978; 100:7101–7103. Danishefsky SJ, Pearson WH. J. Org. Chem. 1983; 48:3865–3866. Amouroux R. Heterocycles. 1984; 22:1489–1492. Iwata C, Hattori K, Uchida S, Imanishi T. Tetrahedron Lett. 1984; 25:2995–2998. Cremins PJ, Wallace TW. J. Chem. Soc. Chem. Commun. 1986:1602–1603. Bernet B, Bishop PM, Caron M, Kawamata T, Roy BL, Ruest L, Soucy P, Deslongchamps P. Can. J. Chem. 1985; 63:2814–2818. Yeates C, Street SDA, Kocienski P, Campbell SF. J. Chem. Soc. Chem. Commun. 1985:1388–1389. Diez-Martin D, Grice P, Kolb HC, Ley SV, Madin A. Tetrahedron Lett. 1990; 31:3445–3448. Kurth MJ, Olmstead MM, Rodriguez MJ. J. Org. Chem. 1990; 55:283–288. Friesen RW, Sturino CF. J. Org. Chem. 1990; 55:5808–5810. Dubois E, Beau JM. Tetrahedron Lett. 1990; 31:5165–5168. Jeong JU, Fuchs PL. J. Am. Chem. Soc. 1994; 116:773–774. Boyce RS, Kennedy RM. Tetrahedron Lett. 1994; 35:5133–5136. Holson EB, Roush WR. Org. Lett. 2002; 4:3719–3722. [PubMed: 12375927]
- For asymmetric variants, see: Uchiyama M, Oka M, Harai S, Ohta A. Tetrahedron Lett. 2001;
   42:1931–1934. Coric I, List B. Nature. 2012; 483:315–319. [PubMed: 22422266] Sun Z, Winschel GA, Borovika A, Nagorny P. J. Am. Chem. Soc. 2012; 134:8074–8077. [PubMed: 22545651]
- 11. Cameron MA, Cush SB, Hammer RP. J. Org. Chem. 1997; 62:9065-9069.
- 12. Friesen RW, Sturino CF, Daljeet AK, Kolaczewska A. J. Org. Chem. 1991; 56:1944–1947.
- 13. Paquette LA, Schulze MM, Bolin DG. J. Org. Chem. 1994; 59:2043–2051.
- 14. Gallier F, Hussain H, Martel A, Kirschning A, Dujardin G. Org. Lett. 2009; 11:3060–3063. [PubMed: 19537770]
- 15. Muchowski JM, Hess P. Tetrahedron Lett. 1988; 29:777-780.
- 16. See Supporting Information for full details.
- Lopez-Perez A, Robles-Machin R, Adrio J, Carretero JC. Angew. Chem. Int. Ed. 2007; 46:9261– 9264.
- Inglis GR, Schwarz JCP, McLaren L. J. Chem. Soc. 1962:1014–1019. Takiura K, Honda S. Carbohydr. Res. 1972; 21:379–391. (c) General review: Chatt J. Chem. Rev. 1951; 48:7–43.

19. The optical rotation of synthetic D-acortatarin A (14),  $[\alpha]_D^{19}$ : + 200 (c 0.4, MeOH), matched that of an authentic sample,  $[\alpha]_D^{19}$ : + 199 (c 0.4, MeOH), confirming the revised absolute stereochemical assignment as 2-deoxy-D-*ribo* (refs. 5, 6).

- 20. The optical rotation of synthetic acortatarin B (**19**),  $[\alpha]_D^{27}$ : -92.7 (c 0.1, MeOH), matched that of an authentic sample,  $[\alpha]_D^{27}$ : -92.9 (c 0.1, MeOH). Examination of the NOESY spectrum of acortatarin B, in comparison to the original ROESY spectrum (ref 1) suggests that mis-assignment of the relative C2–C3 stereochemistry was due to assignment of ambiguous C2-H/C5-H2 crosspeaks, and to non-assignment of an ambiguous C8-H/C5-H crosspeak (Figure S4). Notably, in the structural revision paper (ref 5), C2-H/C5-H2 ROESY crosspeaks also appear but were apparently discounted in favor of clear C5-H/C8-H2 crosspeaks. The reported 7.7 Hz C2-H/C3-H coupling constant is also more consistent with a 2,3-*trans* relationship: Lemieux RU, Stevens JD. Can. J. Chem. 1966; 44:249–262.
- 21. In contrast to 6-membered ring spiroketals, the conformational flexibility of 5-membered rings makes such thermodynamic preferences difficult to predict *a priori* based on anomeric stabilization: Deslongchamps P, Rowan DD, Pothier N, Sauve T, Saunders JK. Can. J. Chem. 1981; 59:1105–1121. Tlais SF, Dudley GB. Org. Lett. 2010; 12:4698–4701. [PubMed: 20860404]
- 22. (a) Gallimore AR, Stark CBW, Bhatt A, Harvey BM, Demydchuk Y, Bolanos-Garcia V, Fowler DJ, Staunton J, Leadlay PF, Spencer JB. Chem. Biol. 2006; 13:453–460. [PubMed: 16632258] (b) Takahashi S, Toyoda A, Sekiyama Y, Takagi H, Nogawa T, Uramoto M, Suzuki R, Koshino H, Kumano T, Panthee S, Dairi T, Ishikawa J, Ikeda H, Sakaki Y, Osada H. Nat. Chem. Biol. 2011; 7:461–468. [PubMed: 21642985]
- 23. For a review on nonanomeric spiroketals, many of which are contrathermodynamic, see: Aho JE, Pihko PM, Rissa TK. Chem. Rev. 2005; 105:4406–4440. [PubMed: 16351049]

**Figure 1.** Original<sup>1</sup> and revised<sup>5</sup> structures of the acortatarins.

**Figure 2.** Retrosynthetic analysis of acortatarins A and B (original structures) via key pyrrologlycal intermediates **1**.

L-thymidine

3

Figure 3. Synthesis of key pyrrologlycal intermediate  $10 \text{ from } \text{\tiny D-thymidine}$  and pyrrole dicarboxaldehyde 9.

Figure 4. Synthesis of acortatarin A (14) via mercury-mediated spirocyclization of pyrrole monoalcohol 11. Acid equilibration of spiroketals 12–15 favors the  $\alpha$ -spiroketals.

Synthesis of acortatarin B (19) via epoxidation and reductive spirocyclization of pyrrole dicarboxaldehyde 10. Acid equilibration of spiroketals 17–20 favors the  $\alpha$ -spiroketals.

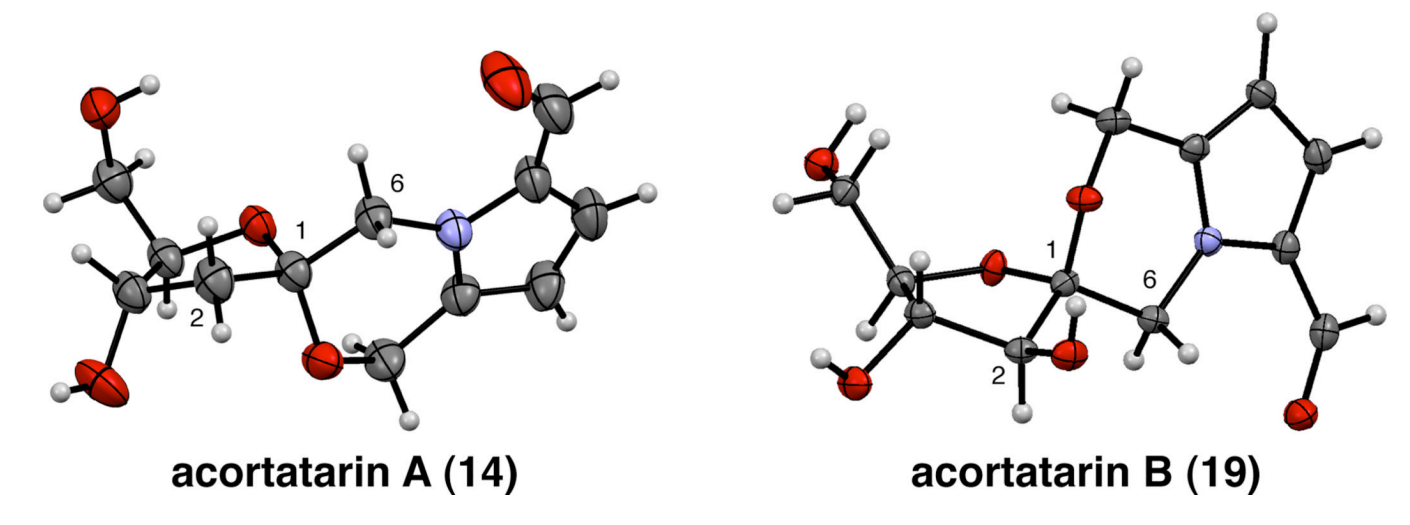


Figure 6. Crystal structures of acortatarin  $A^1$  and acortatarin B reveal distinct ring conformations and double anomeric stabilization. 50% probability ellipsoids shown for heavy atoms.

Wurst et al.

Mercury-mediated spirocyclizations of glycal  $\mathbf{11.}^{16}$ 

				proc	product ratio $^b$	$ti0^{b}$
entry	$reagent^a$	solvent	<i>t</i> (h)	11	12	13
-	Hg(OAc) <sub>2</sub>	THF	1.5	0	19	33
2	$Hg(TFA)_2$	THF	0.5	30	24 <i>c</i>	16
33	$Hg(OAc)_2$	DMF	1.5	10	53	37
4	$Hg(OAc)_2$	hexane	1.5	17	55	28
5	$Hg(OAc)_2$	toluene	1.5	18	54	28
9	NaHMDS; $Hg(OAc)_2$	THF	0.5	10	70	20
7	NaHMDS; $Hg(OAc)_2$	THF	1.5	0	83	17
∞	NaHMDS; $Hg(OAc)_2$	THF	ю	0	85	15
6	NaHMDS; Hg(OAc) <sub>2</sub>	THF	9	0	96	10
10	NaHMDS; $Hg(OAc)_2$	THF	25	0	06	10

<sup>&</sup>lt;sup>a</sup>Base if indicated, –78 °C, 15 min; HgX2, 0 °C  $\rightarrow$  rt; NaBH4, 0 °C.

Page 12

 $<sup>^{</sup>b}$  Determined by  $^{1}$  H-NMR.

<sup>&</sup>lt;sup>c</sup>Additional 30% Ferrier rearrangement-derived 2,3-dehydro-α-spiroketal. (HMDS = hexamethyldisilazane.)

Wurst et al.

Table 2

Reductive spirocyclizations of glycal epoxide 16.

					٦	produc	product ratio $^e$	96
entry	reagent <sup>a</sup>	solvent	temp ( $^{\circ}$ C) $t$ (h)	<i>t</i> (h)	17	18	21	22
-	$NaBH_4^{b}$	МеОН	0 ← 8∠-	1.5	0	0	0	100
2	$\mathrm{NaBH_4}^b$	THF	$-78 \rightarrow 0$	1.5	51	0	13	0
$\epsilon$	$\mathrm{Et_3SiH}^d$	neat	$0 \rightarrow 25$	24	0	0	100	0
4	NaBH $_3$ CN, HCI $^{\mathcal{C}}$	THF	$0 \leftarrow 8L$	1.5	0	42	15	0
S	NaBH(OAc) <sub>3</sub> d	THIF	$0 \leftarrow 8L$	1.5	0	0	0	100
9	${ m LiEt_3BH}^d$	THF	-78	0.5	3	omple	complex mixture	ıre
7	$ ext{L-Selectride}^d$	THF	0←8∠−	12	3	omple	complex mixture	ıre
∞	$\mathrm{Bu}_{4}\mathrm{NBH}_{4}{}^{b}$	$\mathrm{CH}_2\mathrm{Cl}_2$	$-78 \rightarrow 25$	3	78	0	6	0
6	$\mathrm{Bu_4NBH_4}^b$	$\mathrm{CH}_2\mathrm{Cl}_2$	$0 \rightarrow 25$	8	83	•	•	0

 $<sup>^2\</sup>mathrm{Glycal}~\mathbf{10}$  treated with DMDO, CH2Cl2, 0 °C, 1 h, then reductant added in solvent indicated.

b.3 equiv.

 $^{c}$ 0.5 equiv NaBH3CN, 0.1 equiv HCl.

 $d_{1,0,\text{agniv}}$ 

 $^{e}$ Determined by  $^{1}$ H-NMR; remainder hydrolyzed 16.

Page 13